

Design, Optimization and Prototype of a Multi-Phase Fractional Slot Concentrated Windings Surface Mounted on Permanent Magnet Machine

Amir Nekoubin¹, Jafar Soltani^{2*}, Milad Dowlatshahi³

1- 2-3- Department of Electrical Engineering, Khomeinishahr Branch, Islamic Azad University, Khomeinishahr/Isfahan, Iran.
Email: jsoltani@iaukhsh.ac.ir (Corresponding author)

Received: December 2019

Revised: March 2020

Accepted: June 2020

ABSTRACT:

The multi-phase permanent-magnet motors are suitable choices for certain purposes like aircrafts, marine, and electric vehicles due to the fault tolerance and high-power density capabilities. The paper aims to design and prototype an optimized five-phase fractional slot concentrated windings surface mounted permanent magnet motor. To optimize the designed multi-phase motor, a multi-objective optimization technique based on the genetic algorithm method has been applied. The machine design objectives are to minimize mass and loss, subsequently, to determine the best choice of the designed machine parameters. Afterwards, 2-Dimensional Finite Element Method (2D-FEM) has been used to verify the performance of the optimized machine. Finally, the optimized machine has been prototyped. The results of the prototyped machine have validated the results of the theoretical analyses of the machine, and accurate consideration of the parameters improved the performance of the machine.

KEYWORDS: Multi-Phase Machine, Optimization Technique, Permanent-Magnet, Finite Element Technique.

1. INTRODUCTION

A multi-phase motor has several advantages that make this motor preferable to three-phase motors. Multiphase motors can operate under fault condition by using the healthy phases [1-5]. The ability to reduce amplitude and boost the frequency of torque ripple, and the minimization of the stator current per phase without developing the voltage per phase, are the other merits of multiphase motors [6-8]. By adding a number of phases, it is also feasible to develop the torque per RMS ampere for the same volume machine [9-11]. A multiphase motor is a suitable choice for use where high reliability is needed such as in aircraft, marine, and electric vehicles [12-14].

Permanent magnet synchronous motors with Fractional-Slot Concentrated Windings (FSCW) have higher slot fill factor and lower end windings. In addition, the phase's mutual inductances are decreased remarkably. These features enhance the power density of the machine and efficiency. Further, cogging torque will be diminished [3].

Sadeghi [15], have introduced an optimal design of a five-phase Halbach permanent-magnet motor in order to achieve high efficiency, high torque, and high acceleration. The proposed optimal design was

validated through finite-element analysis. It is shown that the optimized multi-phase PM machine offers good performance.

In [16,] a five-phase Fault-tolerant Permanent Magnet Synchronous Machine (PMSM) for electric vehicles is investigated and, for getting sinusoidal back-EMF, two typical methods Consisting of rotor Eccentricity and Halbach permanent-magnet array are studied and compared. Also, a PM method is proposed to decrease PM eddy current loss, it is seen that after PM segmentation, the eddy current loss is reduced significantly. The effects of different design variables on torque ripple and torque linearity that should be investigated at the design stage is studied in [17], it is concluded that torque ripple and torque linearity will be improved by reducing electrical loading. Features of a Permanent-Magnet Synchronous Motor (PMSM) are affected significantly by the back-electromotive force waveforms in the motor, which are directly depended on magnet shape. In [18], a FEM model is used to optimize the radius of the magnet with mention to the number of poles, rotor size, and magnet thickness, it is seen that the optimized motor produce very low total harmonic distortion. In another study [19], the new design optimization technique of Interior

Permanent Magnet (IPM) synchronous motors based on finite the element method is presented. The presented optimization technique is implemented to design two IPM motors for an industrial city electric scooter. It was observed that the simulation results are effective and confirm the proposed technique.

In [20], a new surrogate-assisted multi-objective optimization algorithm is introduced. The introduced algorithm is employed to an optimal design process of a three-phase IPM motor to decrease the noise, vibration, and cost. It is seen that, the introduced algorithm can reduce the design time and effort in IPM motors design using FEM analysis.

In [21], an IPM motor with five-phase and fractional-slot stator is investigated. It is seen that, the presented five-phase motor with fractional slot produces lower torque ripple. In [22], a design model of a three-phase surface-mounted PM motor is presented. The proposed model is suitable to be employed for optimal machine design. There is extra attention to the optimized design of PM motors using genetic algorithm. In [23], a single objective optimization to maximize the torque density for a three-phase surface-mounted PM motor is applied. In this work discontinuous variables such as determination of steel type, Permanent-Magnet (PM) type, and conductor type are also regarded. It is found that, the optimized motor produces high torque density.

Multi-objective genetic algorithms consist of two types, non-elitist and elitist. The elitist strategies are completely applicable because they effectively identify and retain the non-dominated individuals [24-25].

To promote the performance of multi-phase machine design, optimization of the machine is necessary. In this work, the elitist non-dominated sorting GA (NSGA-II) strategy is employed to optimize the multi-phase PM machine. Then, the optimized machine is verified by a FEM model. Finally, the optimized five-phase, surface-mounted PM machine (SPMSM) is prototyped. Thus, the main contributions of this paper are: 1) to design and optimize multi-objectively a five-phase fractional slot concentrated windings surface mounted permanent magnet machine (SPMSM) based on the elitist non-dominated sorting GA (NSGA-II) strategy and determination of the best choice of the designed machine parameters; 2) Two-Dimensional Finite Element Method (2D-FEM) analysis to attest the acting of the optimized motor; 3) prototyping a FSCW 20-slot/ 22-pole five-phase, surface-mounted PM machine (SPMSM).

2. DESIGN OF FIVE-PHASE PMSM MACHINE

The winding factors and MMF harmonic components of FSCW motor are mainly indicated by

Slot/pole combination. Also, other chrectrestics of the motor like ripple torque, net radial force and rotor loss, are affected. Hence, determining an optimized slot/pole combination is fundamental in the motor design steps.

The main component of winding factors for possible slot/pole combination of 5-phase machine is Computed and shown in Table 1.

Table 1. Main winding factors of the multi-phase motor.

s/p	2	4	6	8	12	14	16	18	20	22	24
5	0.58	0.951	0.95	0.58	0.58	0.95	0.95	0.58	-	0.58	0.95
10	-	0.58	0.80	0.95	0.95	0.80	0.58	0.30	-	0.30	0.58
15	0.20	0.40	0.58	0.73	0.95	0.98	0.98	0.95	-	0.73	0.58
20	-	-	0.44	0.58	0.80	0.88	0.95	0.97	-	0.975	0.95
25	0.12	0.24	0.36	0.47	0.67	0.75	0.81	0.89	0.95	0.96	0.98
30	-	0.20	-	0.40	0.58	0.65	0.73	0.80	-	0.90	0.95
35	0.08	0.17	0.26	0.34	0.50	0.58	0.64	0.71	-	0.82	0.86
40	-	-	0.22	-	0.44	0.51	0.58	0.69	-	0.74	0.80
45	0.06	0.13	0.20	0.27	0.40	0.41	0.52	0.58	-	0.68	0.73
50	-	0.12	0.18	0.24	0.36	0.41	0.47	0.48	0.58	0.62	0.67

From the results of Table .1, it can be concluded that 20-slot/ 22-pole combination has the highest winding factors among other combinations.

According to all the conditions connected to fraction slot winding, double layer FSCW 20-slot/ 22-pole Configuration is considered for designing a five-phase surface-mounted permanent-magnet machine.

The initial design of the machine according to the correlation between the machine design specification and the machine geometrical dimensions based on an analytical method is presented in this part. The geometry of a permanent-magnet motor is mainly determined on the basis of torque capability requirements. Other criteria affecting the motor dimensioning are the motor speed rating, and the minimum rotor critical speed. The desired output power of the motor to be designed is 1.1kw at the base speed of 1500rpm; thus, the nominal torque to be reached is about 7N/m.

The first harmonic of the air gap magnetic flux density B_{g1} is, [2].

$$B_{g1} = \frac{1}{\pi} \int_{-0.5\alpha_i\pi}^{0.5\alpha_i\pi} B_g \cos\alpha d\alpha = \frac{2}{\pi} B_g \sin \frac{\alpha_i\pi}{2} \quad (1)$$

Where, coefficient α_i is named the pole-shoe arc-to-pole-pitch ratio, B_g is magnetic flux density of the air gap.

Rotor outer diameter R_{ro} is calculated as:

$$R_{ro} = \frac{pB_gNi}{\pi\sigma} \quad (2)$$

Where, p is the number of magnet pole pairs, σ is shear stress. Ni is coils ampere-turns.

The air-gap thickness for p (number of magnet pole pairs) should be expressed as [2].

$$g = 0.18 + 0.006 P_o^{0.4} \quad (3)$$

Where, P_o is the output power in Watts.

The peak value of the stator (armature) line current density (A/m) or specific electric loading is given by, [2].

$$A_m = \frac{2_m \sqrt{2} N I_a}{\pi D_{sin}} = \frac{m \sqrt{2} N I_a}{p \tau} = \frac{m \sqrt{2} N J_a S_a}{p \tau} \quad (4)$$

Where, p is pole pairs and D_{sin} is the stator inner diameter, J_a is the current density in the stator (armature) conductors (A/m²), N is the number of armature turns per phase, I_a is armature current, τ is pole pitch, s_a is the cross section of armature conductors including parallel wires.

The physical size of the motor is formulated as a function of the flux density in the air gap B_g , in the tooth B_t , and in the back iron B_{bi} .

The back-iron thickness h_{bi} is calculated as [2].

$$h_{bi} = \frac{B_g \pi D_{sin}}{2 B_{bi} 2p} \quad (5)$$

The tooth height h_t is expressed as a function of external diameter D_{sout} and internal diameter D_{sin} as [2].

$$h_t = \frac{D_{sout} - D_{sin}}{2} - h_{bi} \quad (6)$$

Then the tooth width b_{tb} is calculated as [2].

$$b_{tb} = \frac{B_g p_s L}{B_t L} = \frac{B_g \pi D_{sin} L}{B_t Q L} \quad (7)$$

Where Q is the number of slots, and L is stator length.

The slot area S_{slot} is expressed as [2].

$$S_{slot} = \frac{\pi}{4Q} [(D_{sout} - 2h_{bi})^2 - D_{sin}^2] - W_t h_t \quad (8)$$

The number of turns per coil for double-layer winding is given by, [2].

$$N_{coil} = \frac{1}{2} \frac{J_c S_{slot} K_{sf}}{I_R} \quad (9)$$

Where, S_{slot} is the slot area, K_{sf} is the slot fill factor, and I_R is the rms phase current.

The volume of all permanent magnets used in a motor is calculated by equation (10), [2].

$$V_M = 2ph_M \omega_M l_M \quad (10)$$

Where, h_M , w_M , and l_M are the height, width, and length of the PM, respectively.

Considering all the flux generated by the permanent magnet is linked with a stator winding, the fundamental component of back EMF can be calculated by [2].

$$E = 4.444 f N_c B_1 K_w \frac{2 \pi D}{\pi p} L \quad (11)$$

Where, B_1 is the first harmonic of the air gap magnetic flux density, f is frequency, N_c is the number of turns per phase and $K_w l$ is the fundamental winding factor, D is stator bore, P is number of poles, and L is active length of the motor.

The electromagnetic torque is formulated as, [3].

$$T_d = \frac{S_e l m \cos \psi}{2 \pi n_s} = \frac{\pi}{4} K_w D_{sin}^2 L B_g A_m \cos \psi \quad (12)$$

Where, K_w is the winding factor and L is active motor length.

Fig. 1 indicates a cross-section of a PM motor with its geometrical dimensions.

Some of more significant considerations for the design of an electric motor are the current density restriction, and the motor temperature limitation, maximum flux densities in the stator teeth and back iron. With regard to the motor concerns and the design considerations, the initial design of the motor, according to the analytical relations, was investigated.

The flowchart in Fig. 2 shows the initial sizing process of the machine.

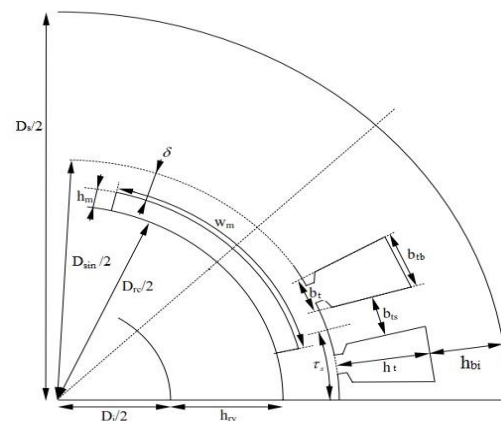


Fig. 1. Cross section of a SMPM.

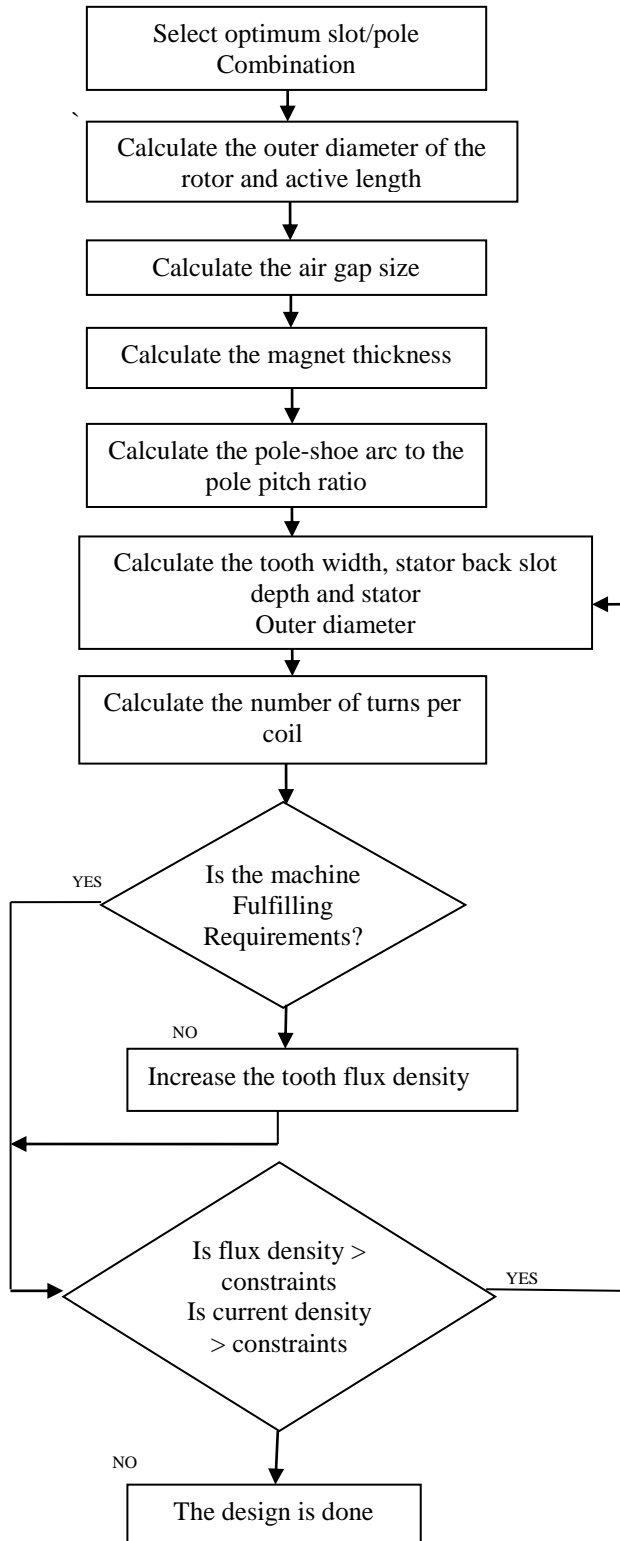


Fig. 2. The flowchart of the initial sizing process of the machine.

The designed five-phase motor with 20-slot and 22-pole is shown in Fig. 3.

The motor parameters derived from the analysis are shown in Table 2 and the analytical results are listed in Table 3.

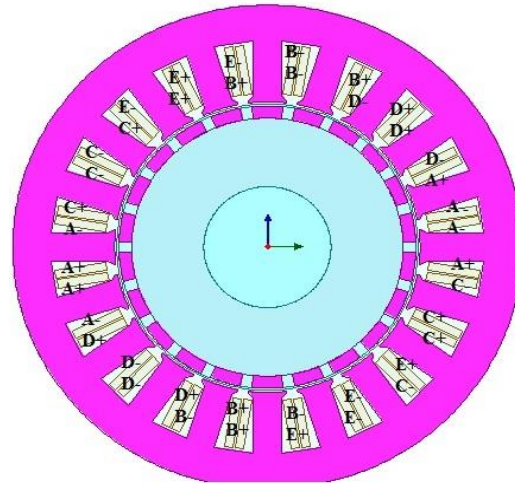


Fig. 3. Five-phase PMSM motor with 20-slot/22-pole.

Table 2. Machine Key Parameters.

Quantity	Values of the five-phase motor
Outer Diameter of rotor	74.4(mm)
Active Length	94.8(mm)
Air Gap	0.5(mm)
Thickness of Magnet	3.56(mm)
Permanent Magnet Fraction	85%
Outer Diameter of stator	127.32(mm)
Slot Depth	15.43(mm)
Stator Back iron depth(mm)	12.5(mm)
Type of Magnet	NdFe35
Type of Steel	M19_24G
Terminal Resistance	7.9838 (ohm)
Wire Diameter	0.5106(mm)
Number of Conductors per Slot	192
Parallel Branches	1
Stacking Factor of Iron Core	0.95

Table 3. Full-Load Data.

Quantity	Values of the five-phase motor
Maximum Line Induced	278.583 (V)
Armature Thermal Load	144.736(A ² /mm ³)
Specific Electric Loading	36.5201(A/mm)
Armature Current Density	4.72008(A/mm ²)
Iron-Core Loss	41.4379(W)
Armature Copper Loss	160.4679(W)
Total Loss	209.9057(W)
Rated Torque	7.00416(N.m)
Total mass	6.75(kg)
Maximum Output Power	4345.23(W)

As we can see from Table 3, the values of the electric loading and armature current density of the machine are reasonable. It can be concluded that the results of the initial design of the machine are in acceptable range. However, the total mass of the machine and the total loss mass are relatively high. In the next part for developing the performance of the machine, a multi-objective optimization will be done.

3. OPTIMIZATION

In this section, optimization for the designed five-phase motor is done. The purpose of this paper is to minimize the power loss and the mass of the machine, subject to considering limitations.

$$\text{Minimize: } g_1 = P_s + P_r + P_c \quad (13)$$

$$\text{Minimize: } g_2 = v_{sl}\rho_s + v_{rb}\rho_r + v_{pm}\rho_m + 5 v_{cd}\rho_c$$

Where, P_c indicates core loss which consists hysteresis loss (P_h) and eddy current loss (P_{edd}).

P_r denotes Resistive loss in the machine, and P_s is Semiconductor loss, and ρ_s, ρ_r, ρ_m and ρ_c denote mass density of the stator, mass density of the rotor, mass density of the permanent magnet and mass density of the conductor, respectively. Moreover, v_{sl} is the total volume of the stator, v_{rb} denotes the total volume of the rotor, v_{pm} is the total volume of the permanent magnets, v_{cd} denotes the total volume of the conductors.

Due to guarantee suitable performance of the machine, a few of limitations on the design are considered. The First limitation is concerned to the machine geometry; it is interested to determine the length of the teeth acceptable compared to their width. The current density of the wire is the next constraint that should not become more than a reasonable value. The next constraints are about the material saturation and the permanent magnet demagnetization. The design variables are determined as the magnet depth, air gap length, magnet fraction, active length, depth of tooth base, and the depth of stator back-iron.

Multi-objective Evolutionary Algorithms (EAs) that employ traditional genetic algorithms have been abolished because of their: 1) High computational complexity of non-dominated sorting (where is the number of objectives and is the population size); 2) non-elitism approach; and 3) the need for specifying a sharing parameter. In this paper, a non-dominated sorting-based multi-objective EA (MOEA), called non-dominated sorting genetic algorithm II (NSGA-II) is used, which moderates all the above three drawbacks. Simulation results on optimization show that the employed NSGA-II is able to find much better spread of solutions and better convergence near the true Pareto-optimal front.

The optimization was planned for a population size of 100 over 100 generations. The first step for the optimization is determining design variables and a range for each of them. These ranges are specified according to the design specifications and the motor design constraints. Table 4 depicts the design variables and ranges for this study.

In the multi-objective technique, all objective functions are optimized at the same time by determining the design parameters. The Genetic Algorithm technique is effectively employed as a powerful method for multi-objective optimization of permanent-magnet machines. This algorithm is consisted of three main steps, initialization, selection, and reproductions. An initial population is produced randomly or according to expert data in the first step. Over an optimization objective function, the fitness of each individual in this population is inspected. For choosing the parents a selection method is employed to the initial population. A new population is generated by applying the genetic operators to parents. To avoid ignoring elite individuals in each population elitist rules are also used. This method is repeated until optimal parameter quantities are reached.

In this paper, the objectives are to minimize the power loss and the mass of the machine, subject to considering limitations.

Table 4. Design Variables Ranges.

Quantity	Min	Max
Air Gap (mm)	0.3	0.8
Magnet depth(mm)	1	5
Magnet Fraction	0.05	0.95
Active length(mm)	20	120
Stator Back iron depth(mm)	1	20
Depth of tooth base (mm)	1	25

3.1. Optimization Results

The multi-objective optimization is used to optimize two objectives at the same time. This causes to a set of so-called *Pareto* optimal results. Fig. 4 shows the result of the multi-objective optimization between mass and loss for the five-phase motor.

For the designed five phase motor, it is observed that, as the mass changes from 3.7 to 9.5 kg, the power loss decreases from 350 Watt to less than 75 W. Loss components versus mass are shown in Fig. 5. Stator resistance loss decreases remarkably with mass but, semiconductor loss and Core loss are approximately steady as mass changes. In fact, the conductor mass goes up as the total mass increases.

The optimized variables and the design results of one of the designs of the pareto-optimal front are listed in Table 5 and Table 6, respectively. It is observed that the specific electric loading and armature Current density are in acceptable values. The core loss and armature copper loss are decreased. Also, it is observed that the total weight is reduced significantly. Therefore, proper multi-objective optimization is applied.

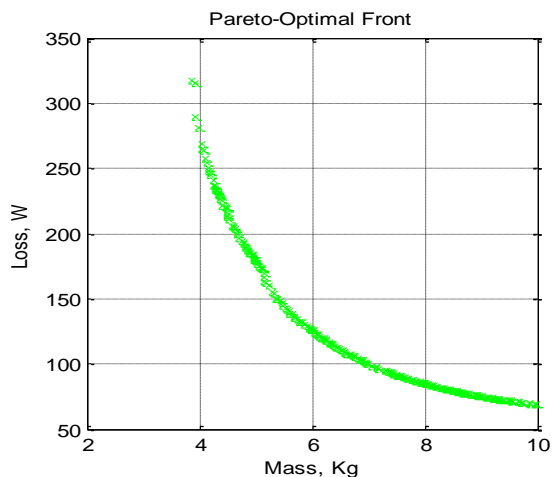


Fig. 4. Pareto-optimal front result for the five-phase motor.

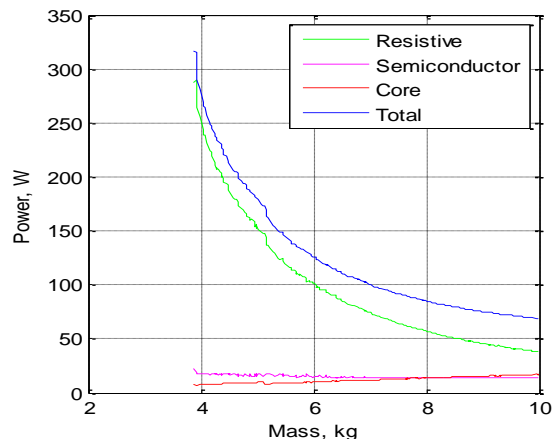


Fig. 5. Power loss components versus mass for the five-phase motor.

Table 5. The optimized design variables.

Quantity	Value	Symbol
Air Gap (mm)	0.495	g
Magnet depth(mm)	3.15	h_m
Magnet Fraction	88	y_a
Active length(mm)	89.76	L
Stator Back iron depth(mm)	23.96	h_{bi}
Depth of tooth base (mm)	13.45	h_t

Table 6. Pareto-Optimal Front Results.

Quantity	Values of the five-phase motor
Maximum Line Induced	282.537 (V)
Armature Thermal Load	99.819(A ² /mm ³)
Specific Electric Loading	19.8125(A/mm)
Armature Current Density	5.0201 (A/mm ²)
Iron-Core Loss	31.4379(W)
Armature Copper Loss	134.4679(W)
Total Loss	176.9057(W)
Rated Torque	7.40416(N.m)
Total mass	5.76(kg)
Maximum Output Power	4693.83 (W)

4. NUMERICAL MODELLING OF PMSM MOTOR

The initial design was performed according to the analytical equations of the electric machine. In this section, a finite-element analysis was employed to verify the model accuracy. A comparison was done to verify the optimized variables of the machine concluded from the analytical method and the FEM model.

4.1. Flux Density Distribution

The flux density distribution as a result of the PM rotor poles of five-phase motor is shown in Fig. 6. It is observed that flux density in tooth (1.355T) and back iron (1.11T) is in reasonable range and the five-phase motor will not be saturated.

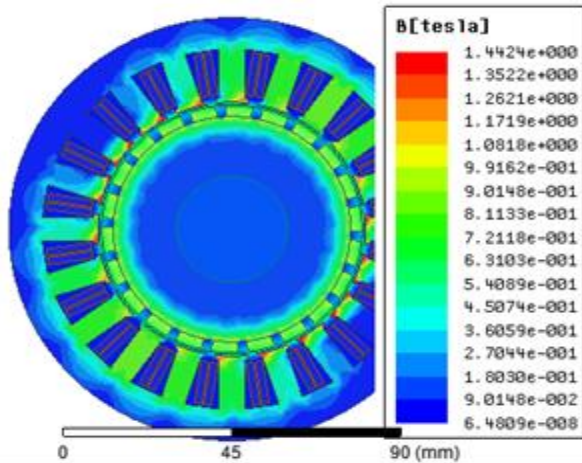


Fig. 6. The flux density distribution of the five-phase motor.

Leakage flux means that there are flux lines that come out from one magnet, enters the stator tooth, but come back to another magnet without coupling with the winding. In Fig. 7, no such flux lines are seen, which indicates that the leakage flux is negligible. Therefore, it is possible to neglect leakage permanent magnet flux and to employ the relation (2) to express back EMF.

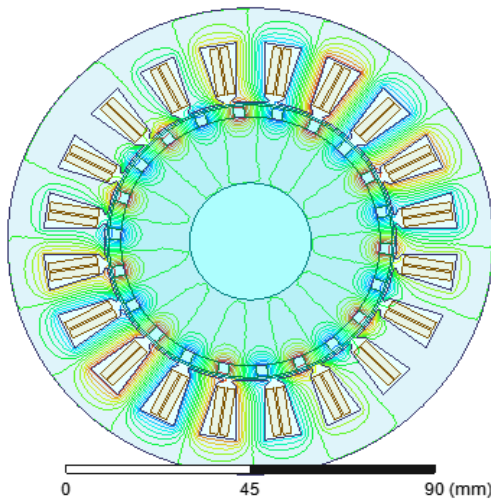


Fig.7. The flux density distribution of the five-phase motor.

4.2. Back Emf

Transient simulation with MAXWELL-2D is done to calculate back-Emf of the optimized motor when the

rotor has its rated speed (1500 rpm). As we can see in Fig. 8, due to slot/ pole combination was selected properly, the back-emf waveforms are completely sinusoidal and their harmonics are eliminated remarkably. The results show acceptable agreement between the analytical calculations and FEM method.

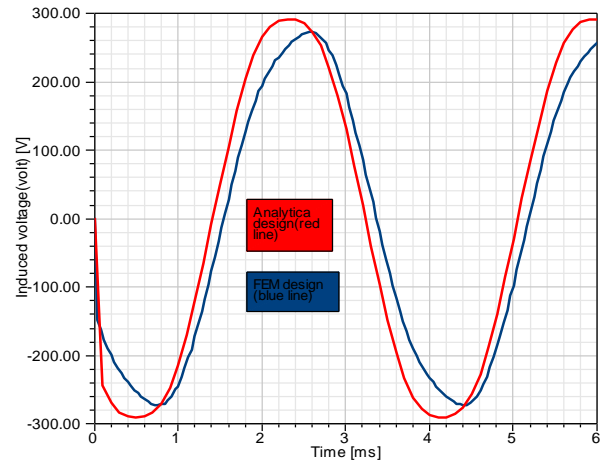


Fig.8. Back EMF calculations at rated speed.

4.3. Electromagnetic Torque

The electromagnetic torque of five-phase motor during full-load condition for the analytical design and the FEA method is shown in Fig. 9. The average torque of the five-phase motor is 7.2 N.m. It should be considered that the analytical design method only implements the fundamental of the air-gap magnetic field and thus the resulting torque is an average value without pulsations. However, this average agrees with the average value of the FEA method.

Finite element analysis results are employed to validate the optimized motor. The results are depicted in Table 7. From the results, it is understood that the inaccuracy is below 5% and it is concluded that the FEM method confirms the accuracy of the optimized design.

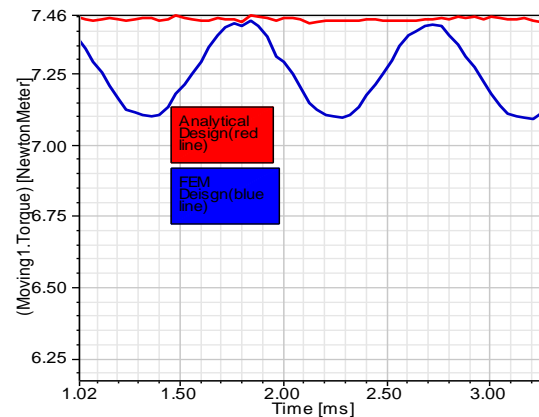


Fig. 9. Electromagnetic torque of the five-phase SPMSM Motor.

Table 7. Comparison of results for five- phase motor.

Quantity	Optimized design	FEM
Maximum Line Induced	282.537 (V)	281.167 (V)
Armature Thermal Load	99.819(A ² /mm ³)	104.736(A ² /mm ³)
Specific Electric Loading	19.8125(A/mm)	20.5201(A/mm)
Armature Current Density	5.0201 (A/mm ²)	5.42008(A/mm ²)
Iron-Core Loss	31.4379(W)	32.765
Armature Copper Loss	134.4679(W)	136.378
Total Loss	176.9057(W)	179.7098(W)
Rated Torque	7. 416(N.m)	7.061(N.m)
Total mass	5.76(kg)	5.91kg)
Maximum Output Power	4693.83 (W)	4678.93 (W)

4.5. Thermal Analysis of the Designed Machine

It is essential to have enough information about the temperature distribution in the motor. FEA is a reliable thermal analysis tool for electrical motors. The thermal distribution of the optimized five-phase motor is shown Fig. 10. For the designed SMPM operation, the main heat sources are the stator copper loss and the stator core loss. As we can see from Table 8, all parts of the optimized motor are operating in acceptable temperature.

Table 8. The Result of thermal analysis of the designed five- phase motor.

Part	Temp [C]
Rotor	98.3872
Winding slot	119.7644
Stator yoke	105.9711
Stator teeth	107.5407

4.6. Prototype and Experiment

The optimized FSCW five-phase, surface-mounted PM machine with 20-slot/ 22-pole is prototyped and tested for validation.

The 22 poles rotor, the stator core with the windings and the prototyped machine is shown in Fig. 11, and Fig. 12 shows the experimental setup.

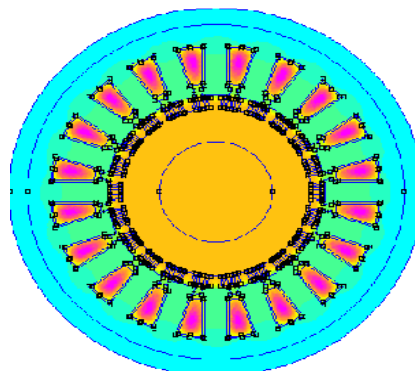


Fig. 10. The thermal distribution of the optimized five-phase motor.



Fig. 11. Rotor core, Stator core with windings and prototyped machine.

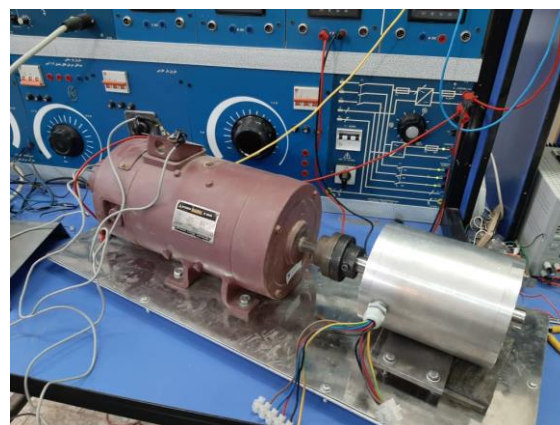


Fig. 12. Experimental setup.

The experimental back-emf of the prototyped machine at the rated speed of 1500r/min is shown in Fig. 13. It could be concluded from Fig.13 that the value and waveform of lab measured back-emf of the

prototype five-phase machine are approximately the same as theoretical measurements.

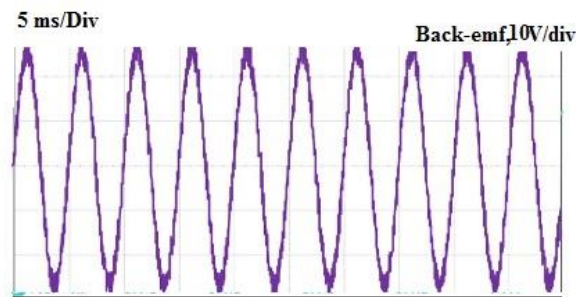


Fig.13 The experimental back-emf of the prototyped machine at the rated speed of 1500r/min

5. CONCLUSION

In this paper, a five-phase surface-mounted permanent-magnet motor was designed, optimized and prototyped. To optimize the designed motors, multi-objective optimization based on a genetic algorithm method was used. Two-Dimensional Finite Element Method (2D-FEM) was used to verify the performance of the optimized machine. Finally, the optimized machine is prototyped. It was concluded that the results of the prototyped machine validate the results of theoretical analyses of the machine. Also, it was seen that multi-phase motor can produce acceptable electromagnetic torque and back-EMF and cogging torque.

REFERENCES

- [1] Gang .Li, Bo Ren, Zi Qiang. Zhu, “Design guidelines for fractional slot multi-phase modular permanent magnet machines,” *IET Electr. Power Appl.*, Vol.11, No. 6, pp. 1023–1031, Nov. 2017.
- [2] A.M. EL-Refaie, Manoj Shah, J.P. Alexander, S. Galitoto, Kum-Kang Huh, W.D. Gerstler., “Rotor End Losses in Multi-Phase Fractional-Slot Concentrated-Winding Permanent Magnet Synchronous Machines,” *IEEE Transactions on Industry Applications*, Vol. 47, No. 5, pp.2066-2074., sep.2011.
- [3] M. EL-Refaie., “Fractional-Slot Concentrated-Windings Synchronous Permanent Magnet Machines: Opportunities and Challenges,” in *IEEE Transactions on Industrial Electronics*, Vol. 57, No. 1, pp. 107-121, Jan. 2010.
- [4] J. S. Choi and J. Yoo., “Structural topology optimization of magnetic actuators using genetic algorithms and on/off sensitivity,” *IEEE Trans. Magn.*, Vol. 45, No. 5, pp. 2276–2279, Feb. 2009.
- [5] Sarikhani and O. A. Mohammed., “Multiobjective design optimization of coupled PM synchronous motor-drive using physics-based modeling approach,” *IEEE Trans. Magn.*, Vol. 47, No. 5, pp. 1266–1269, Sep. 2011.
- [6] J. Cros and P. Viarouge, “Synthesis of high performance PM motors with concentrated

- windings,” *IEEE Trans. Energy Convers.*, Vol. 17, No. 2, pp. 248–253, Jun. 2002.
- [7] Z. Q. Zhu and D. Howe., “Instantaneous magnetic field distribution in brushless permanent magnet motors, part III: Effect of stator slotting,” *IEEE Trans. Magn.*, Vol. 29, No. 1, pp. 143–151, Jan. 1993.
- [8] B. Proca, A. Keyhani, A. El-Antably, W. Lu, and M. Dai., “Analytical model for permanent magnet motors with surface mounted magnets,” *IEEE Trans. Energy Convers.*, Vol. 18, No. 3, pp. 386–391, Sep. 2003..
- [9] M. Refaie, T. M. Jahns, and D. W. Novotny., “Analysis of surface permanent magnet machines with fractional slot concentrated windings,” *IEEE Trans. Energy Convers.*, Vol. 21, No. 1, pp. 34–43, Mar. 2006.
- [10] H. Akita, Y. Nakahara, N. Miyake, and T. Oikawa, “New core structure and manufacturing method for high efficiency of permanent magnet motors,” in *Conf. Rec. IEEE IAS Annu. Meeting*, Salt Lake City, UT, Oct. 2003, Vol. 2, pp. 367–372.
- [11] M. Refaie and T. M. Jahns, “Optimal flux weakening in surface PM machines using fractional slot concentrated windings,” *IEEE Trans. Ind. Appl.*, Vol. 41, No. 3, pp. 790–800, May/June. 2005.
- [12] J. T. Chen and Z. Q. Zhu, “Winding configurations and optimal stator and rotor pole combination of flux-switching PM brushless AC machines,” *IEEE Trans. Energy Convers.*, Vol. 25, No. 2, pp. 293–302, 2010.
- [13] K. Yong, S. C. Hong, S. K. Chang, and S. S. Pan, “A back EMF optimization of double layered large-scale BLDC motor by using hybrid optimization method,” *IEEE Trans. Magn.*, Vol. 47, No. 5, pp. 998–1001, 2011.
- [14] S. Sadeghi, L. Parsa, “Multiobjective Design Optimization of Five-Phase Halbach Array Permanent-Magnet Machine,” *IEEE Trans. Magn.*, Vol. 47, No. 6, pp. 828–837, Jan.2011.
- [15] heng.P, Sui.Y, Zhenxing.F, Wu, “Investigation of a Five-Phase 20-Slot/18-Pole PMSM for Electric Vehicles,” 17th International Conference on Electrical Machines and Systems, Hangzhou, China (ICEMS), Oct 2014, pp. 22–25.
- [16] M. S. Islam, R. Islam and T. Sebastian, “Experimental Verification of Design Techniques for Permanent-Magnet Synchronous Motors for Low-Torque-Ripple Applications,” *IEEE Trans. Ind. Appl.*, Vol. 47, No. 1, pp. 28–37, Jan. 2011.
- [17] Y. Li, J. Xing, T. Wang, and Y. Lu, “Programmable Design of Magnet Shape for Permanent Magnet Synchronous Motors With Sinusoidal Back EMF Waveforms,” *IEEE Trans. Mag.*, Vol. 44, No. 9, pp. 18–25, sep. 2008.
- [18] F.Parasiliti, M.Villani, S.Lucidi, “Finite-Element-Based Multiobjective Design Optimization Procedure of Interior Permanent Magnet Synchronous Motors for Wide Constant-Power Region Operation,” *IEEE Trans. Mag.* Vol. 6, No. 10, pp. 211-219, oct.2012.
- [19] Lim.D, Kyung.Y, Sang.J, “Optimal Design of an Interior Permanent Magnet Synchronous Motor by

- Using a New Surrogate-Assisted Multi-Objective Optimization,” *IEEE Trans. Mag.* Vol. 51, No. 11, pp. 11-19, Feb. 2015
- [20] L.Parsa, A. Toliyat, “Five-Phase Interior Permanent-Magnet Motors With Low Torque Pulsation”, *IEEE Trans. Ind Appl.* Vol. 43, No. 1, pp. 128–137, sep. 2007.
- [21] N. Cassimere and S. D. Sudhoff, “Population based design of surfacemounted permanent magnet synchronous machines”, *IEEE Trans. Ene.*, Vol. 24, No. 2, pp. 41-48, 2009.
- [22] S. D. Sudhoff, J. Cale, B. N. Cassimere, and M. D. Swinney, “Genetic algorithm design of a permanent magnet synchronous machine”, in Proc. IEEE Int. Conf. Electr. Mach. Drives, 2005, pp. 1011–1019.
- [23] K. Deb.: ‘*Multi-Objective Optimization Using Evolutionary Algorithms*’, (New York: Wiley, 2001)
- [24] J. Kim, D. Cho, H. Jung, C. Lee, “Niching genetic algorithm adopting restricted ompetition selection combined with pattern search method”, *IEEE Trans. Mag.*, Vol. 38, No. 2, pp. 1001 – 1004, sep. 2002.
- [25] S.D. Sudhoff, Y. Lee, “Energy Systems Analysis Consortium (ESAC) Genetic Optimization System Engineering Tool (GOSET) Version 1.05 Manual,” School of Electrical and Computer Engr., Purdue Univ., West Lafayette, IN 47907,2003.